Pharm Res (2013) 30:1586–1596
DOI 10.1007/s11095-013-0997-4

RESEARCH PAPER

Inhalable Powder Formulation of Pirfenidone with Reduced Phototoxic Risk for Treatment of Pulmonary Fibrosis

Satomi Onoue • Yoshiki Seto • Masashi Kato • Yosuke Aoki • Yoshiki Kojo • Shizuo Yamada

Received: 18 September 2012 / Accepted: 28 January 2013 / Published online: 21 February 2013

ABSTRACT

Purpose Orally-taken pirfenidone (PFD), an idiopathic pulmonary fibrosis drug, often causes severe phototoxicity. Present study aimed to develop a respirable powder formulation for PFD (PFD-RP) to minimize phototoxic risk.

Methods Photochemical properties of PFD were examined using a reactive oxygen species (ROS) assay and photostability testing. PFD-RP was characterized with a focus on photostability, *in vitro* inhalation performance, and the efficacy in antigen-sensitized rats. Pharmacokinetic studies were conducted after oral and intratracheal administration of PFD formulations.

Results Although PFD solution exhibited photodegradation under simulated sunlight (250 W/m^2), both PFD powder and PFD-RP were photochemically stable. Laser diffraction and cascade impactor analyses on PFD-RP suggested its high dispersion and fine *in vitro* inhalation performance. Inhaled PFD-RP (300 μg-PFD/rat) could suppress antigen-evoked pulmonary inflammation in rats as evidenced by decreases in recruited inflammatory cells and neutrophilia-related biomarkers in the lung. Exposure of PFD to light-exposed tissues (skin and eye) after intratracheal administration of PFD-RP at a pharmacologically effective dose (300 μg-PFD/rat) was 90–130-fold less than that of the oral PFD dosage form at a phototoxic dose (160 mg/kg).

Conclusions PFD-RP might be an attractive alternative to the current oral PFD therapy with a better safety margin.

KEY WORDS inhalation · photostability · phototoxicity · pirfenidone · pulmonary fibrosis

S. Onoue (✉) · Y. Seto · M. Kato · Y. Aoki · Y. Kojo · S. Yamada
Department of Pharmacokinetics and Pharmacodynamics
School of Pharmaceutical Sciences
University of Shizuoka, 52-1 Yada, Suruga-ku
Shizuoka 422-8526, Japan
e-mail: onoue@u-shizuoka-ken.ac.jp

ABBREVIATIONS

8-MOP	8-methoxypsoralen
ANOVA	analysis of variance
AUC	area under concentration *versus* time curve
AUMC	area under moment curve
BALF	bronchoalveolar lavage fluid
EPO	eosinophil peroxidase
ESI-MS	electrospray ionization mass spectrometry
FQ	fluoroquinolones
HPMC	hydroxypropyl methylcellulose
MPO	myeloperoxidase
MRT	mean residence time
OVA	ovalbumin
PBS	phosphate-buffered saline
ROS	reactive oxygen species
RP	respirable powder
SEM	scanning electron microscopy
TMBZ	3,3′,5,5′-tetramethylbenzidine
UPLC	ultra performance liquid chromatography

INTRODUCTION

Pirfenidone (PFD), 5-methyl-1-phenylpyridin-2-one, is a novel anti-fibrotic and anti-inflammatory agent for suppressing the progression of lung, kidney, and hepatic fibrosis and inflammatory events in experimental animal models (1–4). PFD can regulate the activity of TGF-β and TNF-α, leading to the inhibition of fibroblast proliferation and collagen synthesis (5). The detailed mechanism whereby PFD modulates fibrogenesis is still unclear and the biological activities of PFD may be multitargeted. PFD has been clinically used as the first anti-fibrotic drug (Esbriet®, Pirespa®) available for mild-to-moderate idiopathic pulmonary fibrosis (IPF) in Europe, Japan, India, and China (4,6,7). Although PFD

has an attractive therapeutic potential for the treatment of IPF, orally-taken PFD often causes systemic side effects, such as nausea, anorexia, dizziness, rash, hepatic dysfunction, and phototoxicity (6,8,9). In particular, the phototoxic skin response is a well-known adverse effect of PFD treatment and its frequency has been shown to be as much as ca. 50% in a clinical study (8). PFD-induced phototoxicity may be controlled by either dose reductions or the termination of treatment; however, in the clinical study, there were no significant differences in the incidence of phototoxicity between the high-dose (51% in patients with 1.8 g/day of PFD) and low-dose group (53% in patients with 1.2 g/day of PFD).

Phototoxic skin responses can be caused by the combined effects of UV/VIS irradiation and external phototoxic drugs (10), and increasing attention has been drawn to drug-induced phototoxicity because of the gradual expansion of the UV portion in the solar spectrum. Owing to possible reductions in medication compliance, drug-induced phototoxicity is one of the impediments in pharmaceutical development and a number of efforts have been made to avoid drug-induced phototoxic reactions. Theoretically, drug-induced phototoxicity is induced in light-exposed tissues, especially skin (11,12); therefore, control of dermal PFD concentrations with use of appropriate formulation technologies may be of great value for reducing the phototoxic risk of PFD. Recently, several respirable formulation systems have been developed for the treatment of airway inflammation and inhalation therapy could achieve a high drug concentration in the lung with low systemic exposure (13,14). Strategic application of PFD to the respirable formulation system may also lead to successful development of efficacious PFD medications with a wide safety margin, whereas far less is known about the feasibility and pharmacological outcomes of the respirable formulation of PFD.

The present study aimed to design a new respirable formulation system for PFD with the aim of maximizing topical effects in the lung and minimizing the exposure of PFD to light-exposed tissues. Based on results from photostability testing on PFD samples, the respirable powder (RP) formulation of PFD, composed of lactose carriers and a micronized mixture of PFD and erythritol, was developed with a jet mill. The physicochemical properties of PFD-RP were characterized with a focus on morphology by scanning electron microscopy, particle size distribution by laser diffraction analysis, and *in vitro* inhalation performance by cascade impactor experiments. In antigen-sensitized rats, the pharmacological effects of insufflated PFD-RP were assessed upon recruitment of inflammatory cells and neutrophilia-/eosinophilia-related biomarkers in bronchoalveolar lavage fluid (BALF). To verify the photosafety of PFD-RP, comparative pharmacokinetic studies were carried out in rats after intratracheal administration of PFD-RP at pharmacologically effective doses or oral administration of PFD at phototoxic and non-phototoxic doses.

MATERIALS AND METHODS

Chemicals

PFD was kindly provided by Shionogi (Osaka, Japan). Respitose® SV-003 and erythritol were supplied by DMV (Veghel, The Netherlands) and Nikken Chemicals (Tokyo, Japan), respectively. Aluminum hydroxide (alum) gel, horseradish peroxidase, ovalbumin (OVA), and sodium pentobarbital were purchased from Sigma Aldrich (St. Louis, MO). Ammonium acetate, *o*-phenylenediamine (OPD), and trypan blue were bought from Wako Pure Chemical Industries (Tokyo, Japan). 3,3′,5,5′-Tetramethylbenzidine (TMBZ) was bought from Dojindo (Kumamoto, Japan). All other reagents were obtained from commercial sources.

Solar Simulator

Photochemical studies were carried out using an Atlas Suntest CPS+ solar simulator (Atlas Material Technology LLC, Chicago, IL, USA) equipped with a xenon arc lamp (1,500 W). A UV special filter was installed to adapt the spectrum of the artificial light source to that of natural daylight. An irradiation test was carried out at 25°C with an irradiance of 250 W/m^2 (300–800 nm).

Reactive Oxygen Species (ROS) Assay

The ROS assay was originally designed to evaluate the photochemical reactivity of tested chemicals by determining both singlet oxygen and superoxide generated from photo-irradiated chemicals (15). In the present study, the ROS assay was undertaken to clarify the photochemical properties of PFD. Briefly, singlet oxygen was measured in an aqueous solution by spectrophotometrically monitoring the bleaching of RNO at 440 nm using imidazole as a selective acceptor of singlet oxygen. Samples, containing the tested chemical (200 μM), *p*-nitrosodimethylaniline (50 μM), and imidazole (50 μM) in 20 mM sodium phosphate buffer (NaPB) (pH 7.4), were irradiated with simulated sunlight (250 W/m^2) and then UV absorption at 440 nm was measured using a SAFIRE microplate spectrophotometer (TECAN, Männedorf, Switzerland). For the determination of superoxide, samples containing the tested chemical (200 μM) and

nitroblue tetrazolium (NBT, 50 μM) in 20 mM NaPB were irradiated with simulated sunlight for 1 h and reductions in NBT were measured by increases in absorbance at 560 nm using a SAFIRE microplate spectrophotometer (TECAN).

Photostability Testing

For the solid-state stability test, PFD formulations (5 mg) were weighed exactly and spread in a 15 mL clear glass vial over the whole bottom surface. For the solution-state stability study, PFD (5 mg) was weighed in a 15 mL clear glass vial and dissolved in 5 mL of distilled water. Each sample was set in the Suntest CPS+ solar simulator and irradiated with simulated sunlight (250 W/m^2) for the indicated periods. A reference sample protected by aluminum foil was examined under the same conditions. Each solid sample was dissolved in 10 mL of 50% acetonitrile and PFD remaining in the sample was determined with ultra-performance liquid chromatography equipped with electrospray ionization mass spectrometry (UPLC/ESI-MS) analysis. The UPLC/ESI-MS system consisted of a Waters Acquity UPLC^{TM} system (Waters), which included a binary solvent manager, a sample manager, a column compartment, and a Micromass SQ detector connected with Waters MassLynx v 4.1. A Waters Acquity UPLC^{TM} BEH C_{18} (particle size: 1.7 μm, column size: Φ 2.1×50 mm; Waters) was used and column temperature was maintained at 40°C. Samples were separated using a gradient mobile phase consisting of Milli-Q containing 0.1% formic acid (A) and MeOH (B). The gradient condition of the mobile phase was 0–0.5 min, 80% A; 0.5–4 min, 80–25% A (gradient curve: 8); 4–5 min, 5% A; 5–6 min, 80% A, and the flow rate was set at 0.25 mL/min. Analysis was carried out using SIR for specific *m/z*: 186 $[M+H]^+$ for PFD.

Preparation of Respirable Powder Formulations

RP formulations of PFD and OVA (PFD-RP and OVA-RP) were prepared as reported previously (14). PFD or OVA particles and excipients, including lactose or erythritol, respectively, were first ground to fine powders with a pestle and mortar and then milled with an A-O JET MILL (Seishin Enterprise, Tokyo, Japan) at a pusher nozzle pressure and grinding nozzle pressure of 6.0 and 6.5 kg/cm^2G for PFD or 6.0 and 5.5 kg/cm^2G for OVA, respectively. The ratio of PFD or OVA to excipient was 3:2 or 1:400 (w/w), respectively. Micronized PFD and OVA were decompounded with 10-fold lactose (Respitose®, SV-003) and erythritol carrier particles, respectively, in a plastic bag for 3 min and the obtained dry powders of PFD and OVA were stored in a vacuum desiccator until tested. The amount of PFD in the RP formulation was determined by UPLC/ESI-MS analysis as described in the "Photostability Testing" section.

Scanning Electron Microscopy (SEM)

PFD-RP was coated with platinum on a HITACHI Ion Sputter E-1010 (Hitachi, Tokyo, Japan). Representative scanning electron microscopic images of PFD-RP were taken using a VE-7800 scanning electron microscope (Keyence Corporation, Osaka, Japan). For SEM observations, each sample was fixed on an aluminum sample holder using double-sided carbon tape.

Particle Size Distribution

The particle size distribution of PFD-RP was measured using a laser diffraction scattering method with an LMS-2000e (Seishin Enterprise, Tokyo, Japan). PFD-RP was subjected to dry spraying at a pressure of 0.2 MPa for effective dispersion into fine particles and carrier molecules and then particles were calculated.

Cascade Impactor Analysis

The *in vitro* inhalation performance of the RP formulation was assessed according to USP 29 <601> AEROSOLS using an AN-200 system (Shibata Scientific Technology, Tokyo, Japan), consisting of a vacuum pump, mass flow meter, and eight-stage Andersen cascade impactor. Briefly, dry powders were filled into a JP No. 2 hard capsule of hydroxypropyl methylcellulose (HPMC) and the capsule was installed in a JetHaler® (Hitachi Unisia, Kanagawa, Japan) powder inhaler. Dry powder formulations (40 mg) in each capsule were dispersed *via* the device with an inspiration rate of 28.3 L/min for an inhalation time of 10 s×5 times and the collection stages of the impactor (stages 0–7) were washed with purified water. PFD in each solution was determined by UPLC/ESI-MS as described in the "Photostability Testing" section. The fine particle dose (FPD) was defined as the mass of drug particles measuring less than 5.8 μm (particles deposited at stage 2 and lower). The fine particle fraction (FPF) was calculated as the ratio of FPD to the total loaded dose.

Animals and Drug Insufflation

Male Sprague–Dawley rats (7–9 weeks of age; Japan SLC, Shizuoka, Japan), weighing 200–350 g, were housed three per cage in the laboratory with free access to food and water and were maintained on a 12-h dark/light cycle in a room with controlled temperature (24±1°C) and humidity (55±5%).

Animals were fasted for 12 h before experiments. Rats were sensitized by intraperitoneal injection of 100 μg of OVA with 5 mg of alum on days 0, 7, and 14. They were anesthetized with sodium pentobarbital (50 mg/kg, i.p.) and received intratracheal administration of OVA (100 μg/rat) powder at 24 h after the last OVA sensitization. At 1 h before the OVA challenge, PFD-RP (30–1,000 μg-PFD/kg) or PFD-free RP formulation (control-RP) was administered *via* intratracheal insufflation using a PennCentury insufflation powder delivery device (DP-4, INA Research Inc., Nagoya, Japan). A bolus (2 mL) of air from an attached syringe was used to deliver the preloaded powder from the chamber of the insufflator into the airway system of the rats. At 24 h after OVA challenge, rats were exsanguinated *via* the descending aorta under anesthesia with sodium pentobarbital and the lungs were perfused with 30 mL of saline and removed. All procedures used in the present study were conducted in accordance with the guidelines approved by the Institutional Animal Care and Ethical Committee of the University of Shizuoka.

Total Cell Counting in BALF

At 24 h after the OVA challenge, bronchoalveolar lavage fluid (BALF) was collected by washing the airways twice with 5 mL of PBS. BALF was pooled and immediately centrifuged at 112×*g* for 10 min, the supernatant was then removed, and cells were re-suspended with 1 mL of PBS. The total number of cells in BALF upon adding an equal amount of 0.2% trypan blue was counted using a Burker-Turk counting chamber.

Measurement of MPO and EPO Activities

Enzymatic detection of MPO and EPO in BALF was performed in accordance with a previous report (13,16). Briefly, for the MPO measurement, assay mixtures consisted of 40 μL of H_2O_2 (final concentration 0.3 mM) in 80 mM sodium phosphate buffer (pH 5.4) and 50 μL of BALF samples. The reaction was initiated by the addition of 10 μL of TMBZ (final concentration 1.6 mM) in dimethyl sulfoxide at 37°C and stopped after 2 min by the addition of 0.18 M H_2SO_4. Subsequently, optical density was determined at 450 nm. For the detection of EPO activity in BALF, the reaction mixture was prepared by adding 500 μL of OPD (50 mM) to 24.25 mL of Tris buffer (pH8.0), 3 μL of 30% H_2O_2, and 25 μL of Triton X-100. Then, 100 μL of reaction mixture was added to 50 μL of BALF sample in a 96-well plate and incubated for 30 min at room temperature. The reaction was stopped by the addition of 2 M H_2SO_4 and absorbance at 490 nm was measured. A titration curve of horseradish peroxidase was used for the calculation of MPO and EPO activities, which were expressed in arbitrary units. All samples were assayed in duplicate and optical densities in all assays were measured using a Safire microplate reader (Tecan).

Plasma Concentration of PFD After Oral Administration

Rats were anesthetized using pentobarbital (40 mg/kg, i.p.) and a cannula (PE8050, Natsume, Tokyo, Japan) was inserted into the arteria femoralis before PFD was administered orally. Blood samples (approximately 150 μL) were collected from the cannulated arteria femoralis at the indicated times (5, 10, 15, 30, 45 min, 1, 1.5, 2, 3, 4, and 6 h) after oral administration of PFD (30 and 160 mg/kg) or intratracheal administration of PFD-RP (300 μg-PFD/rat). Plasma obtained by centrifugation (10,000×*g*, 10 min, 4°C) was deproteinized by the addition of acetonitrile (plasma : acetonitrile = 2 : 5), and plasma was mixed and centrifuged (2,000 rpm, 1 min, 4°C). Supernatants were filtered and 50% acetonitrile solution containing antipyrine (5 μg/mL), an internal standard, was added (supernatant : nalidixic acid = 9 : 1) for UPLC/ESI-MS analysis as described in the "Photostability Testing" section.

Tissue Deposition of PFD

After oral administration of PFD (30 and 160 mg/kg) or intratracheal administration of PFD-RP (300 μg-PFD/rat), rats were sacrificed at the indicated periods (5, 30 min, 1, 2, 3, 4, and 6 h) by taking blood from the descending aorta under temporary anesthesia with diethyl ether and tissues were then perfused with cold saline from the aorta. The skin, lung, and eyes were dissected and fat and blood vessels were removed by trimming. Tissues were minced with scissors in stoppered test tubes and homogenized by a Cryo-press (CP-100W, Microtech, Chiba, Japan) and Physcotron (Microtech) in 4 mL of acetonitrile. After shaking for 5 min and sonication for 10 min, mixtures were centrifuged (3,000 rpm, 10 min). This extraction was repeated two times with acetonitrile and supernatants were pooled. Samples were evaporated to dryness under a gentle stream of nitrogen at 45°C and residues were dissolved in 50% acetonitrile solution containing antipyrine (500 ng/mL) as an internal standard for UPLC/ESI-MS analysis.

Pharmacokinetic Analysis

Pharmacokinetic characterization in plasma was performed by non-compartmental analysis as implemented in WinNonlin Professional Version 5.2 (Pharsight Corporation,

Mountain View, CA, USA) and that in tissues was carried out by non-compartmental analysis. The elimination rate constant (k_{el}) was estimated by the least square method from the terminal phase. The elimination half-life ($t_{1/2}$) was calculated using the following equation.

$$t_{1/2} = \frac{\ln 2}{k_{el}}$$

Area under concentration *versus* time curve ($AUC_{0\to\infty}$), area under moment curve ($AUMC_{0\to\infty}$), and mean residence time (MRT) were estimated using a trapezoid formula from 0 h to the last measurement time (T), after which the last observed concentration (C_T) and $t_{1/2}$ were used as follows:

$$AUC_{0\to\infty} = \int_0^T Cdt + \frac{C_T}{k_{el}}$$
$$AUMC_{0\to\infty} = \int_0^T t \cdot Cdt + \frac{T \cdot C_T}{k_{el}} = \frac{C_T}{k_{el}^2}$$
$$MRT = \frac{AUMC_{0\to\infty}}{AUC_{0\to\infty}}$$

where C is the observed plasma or tissue concentration (plasma: ng/mL, tissues: ng/g skin) and t equals the measurement time (h).

Statistical Analysis

For statistical comparisons, a one-way analysis of variance (ANOVA) with pairwise comparison by the Fisher's least significant difference procedure was used. A p value of less than 0.05 was considered significant for all analyses.

RESULTS AND DISCUSSION

Photostability Testing on Pirfenidone Formulations

The photochemical reactivity of a drug formulation, as well as its chemical stability, is an important aspect to consider during development, production, storage, and use of pharmaceutical preparations. PFD is a potent UV absorber with a molar extinction coefficient of 6,450 $M^{-1}.cm^{-1}$ (λ_{max}: 313 nm, data not shown) and may be photolabile when it absorbed the photon energy, possibly leading to a loss in its potency. Therefore, in the present study, the photoreactivity of PFD was firstly assessed by a reactive oxygen species (ROS) assay as previously reported by Onoue and Tsuda (15). The ROS assay was established to monitor the generation of ROS, such as singlet oxygen and superoxide, from photoirradiated chemicals (15,17), and ROS generation would be indicative of the photochemical reactivity of tested chemicals (11). Sulisobenzone, a potent UV absorber, has no ability to generate ROS when exposed to simulated sunlight (250 W/m^2; Fig. 1a); therefore, sulisobenzone can be identified to be less photoreactive as reported previously. In contrast, 8-methoxypsoralen (MOP), a known phototoxic and photoreactive chemical, and PFD exhibited potent ROS generation under light exposure. Although 8-MOP slightly exceeded PFD in ROS generation, both chemicals were identified to be photoreactive according to the previously defined threshold [singlet oxygen ($\Delta A_{440\ nm}\ 10^3$): 25; superoxide ($\Delta A_{560\ nm}\ 10^3$): 20] (17,18). From these findings, taken together with observed phototoxicity, PFD would be photoreactive, which raises concerns about its photostability.

In respirable formulation systems, an aerosol of PFD can be produced from both liquid and powder formulations in theory, while the photostability of PFD may limit a viable dosage option. To clarify the photochemical properties in more detail, photostability testing was carried out for powder and liquid forms of PFD using a solar simulator equipped with a Xe lamp (Fig. 1b). None of the PFD samples tested here showed any degradation in chromatographic analysis when they were stored at 25°C for at least 1 h under light protection (data not shown). Exposure of PFD solution to simulated sunlight (250 W/m^2) resulted in the gradual degradation of PFD, and it was likely to follow first-order kinetics with an apparent first-order degradation rate of $0.31 \pm 0.03\ h^{-1}$. In contrast, no significant degradation was observed in PFD powder under the same irradiation conditions. In general, as previously observed in curcumin (19) and coenzyme Q_{10} (20), photosensitive chemicals in a solution state were far more prone to photodegradation than solid samples due to the high permeability of light and increased mobility of photochemically excited molecules and reactive species. On the basis of the photochemical properties of PFD, taken together with previous findings, a nebulizer system using the liquid formulation of PFD may not be suitable for inhalation therapy with PFD from a stability point of view. This could be a rationale for the development of a PFD-loaded RP formulation (PDF-RP), a dry powder inhaler system, in the present investigation.

Respirable Powder Formulation of Pirfenidone

PFD powders were grinded with lactose by the jet-milling system, and then, PFD-RP, a respirable powder formulation of PFD, was obtained by mixing jet-milled PFD particles and Respitose®, a lactose carrier for inhalation therapy. When PFD-RP was exposed to simulated sunlight (250 W/m^2) (Fig. 1b), PFD-RP was found to be stable for at least 1 h, as observed in powder PFD. Thus, an RP approach would surpass the nebulizer system in terms of photochemical stability; therefore, the formulation strategy may be an appropriate delivery option for PFD to treat IPF. However, because of the photoreactive potential of PFD, appropriate UV-light protection may be necessary for the PFD-RP to maintain product quality during long-term storage.

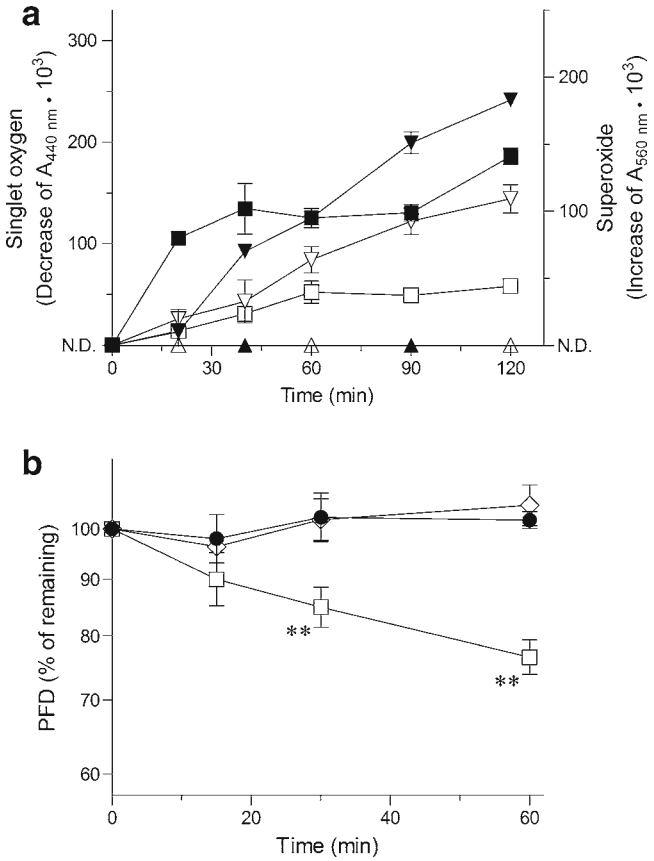

Fig. 1 Photochemical properties of PFD samples. (**a**) Generation of singlet oxygen (*open symbols*) and superoxide (*filled symbols*) from PFD exposed to simulated sunlight (250 W/m^2). □/■, PFD; ▽/▼, 8-MOP; and △/▲, sulisobenzone. Data represent mean±SD of three experiments. (**b**) Photostability data on PFD formulations under exposure to simulated sunlight (250 W/m^2). □, PFD solution; ◇, PFD powder; and ●, PFD-RP. Data represent mean±SD of three experiments. **, $P<0.01$ with respect to the PFD powder.

For better clinical outcomes from inhalation therapy, micronized particles in the RP formulation should be well aerosolized and delivered into respiratory systems. In particular, particle size and the dispersibility of inhalable particles could be key factors when deeply inhaled into the lung and for achieving favorable effects on pulmonary diseases (21). In this context, the physicochemical properties of PFD-RP were assessed with a focus on surface morphology, particle size distribution, and *in vitro* inhalation performance (Fig. 2). The surface morphology of PFD-RP was visualized by SEM (Fig. 2a), demonstrating that micronized PFD particles could be obtained in the form of uniform spherical particles by jet-milling and micronized particles were attached to the surface of lactose carriers without any significant agglomeration. In the laser diffraction analysis of PFD-RP (Fig. 2b) dispersed with pressuring air at 2.0 kg/cm^{2}G, there appeared to be two clear peaks for jet-milled PFD particles and carriers at ca. 7 and ca. 65 μm, respectively. This data suggested the fine dispersion and aerosolization of jet-milled PFD powders under the

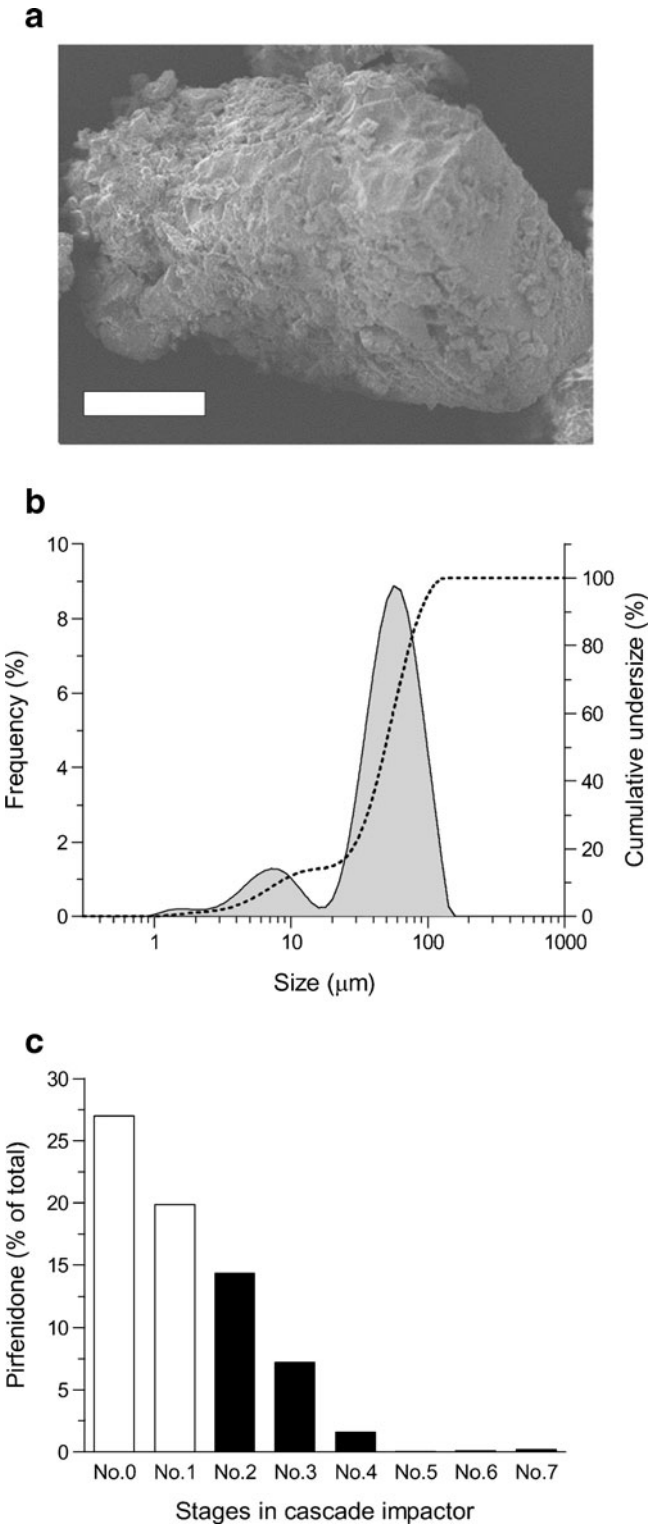

Fig. 2 Appearance and aerosolization efficiency of PFD-RP. (**a**) Scanning electron microscopic images of PFD-RP. Bar represents 20 μm. (**b**) Particle size and aerosolization efficiency of PFD-RP as determined by laser diffraction particle size analysis. PFD-RP was dispersed by dry air at a pressure of 0.2 MPa. *Solid line*, frequency; and *dotted line*, cumulative undersize fraction curve. (**c**) *In vitro* inhalation performance of PFD-RP. Deposition pattern analysis of PFD-RP was conducted using a cascade impactor connecting JetHaler® with an airflow rate of 28.3 L/min.

experimental condition and that jet-milled PFD particles may be micronized well with a mean diameter of ca. 7.0 μm and a SPAN factor of ca. 1.4. The size of a drug particle critically influences lung deposition (22), and the nature of the aerosolized particles is dependent on its mass median aerodynamic diameter (MMAD) that is a function of particle size, shape and density. Aerosols should be neither too large nor too small. According to a previous report (23), the optimal particle size of drugs to achieve a fine delivery to the bronchial tubes and alveolus was ca. 3–9 μm. Inhaled particles with diameter of over 10 μm, such as carrier particles, are deposited in the mouth or oropharynx, being eventually absorbed from the gut. Particles with diameter of less than 0.5 μm can be inhaled into the deep lung but have a high probability of being exhaled before deposition. In this context, the jet-milled PFD particles with mean diameter of ca. 7.0 μm would be delivered to the pulmonary tissues, possibly leading to the topical therapeutic effects, although the carrier particles might be deposited in the mouth. Therefore, the prepared PFD-RP could be theoretically appropriate for inhalation use. The *in vitro* inhalation performance of PFD-RP was further characterized by cascade impactor analysis (Fig. 2c), in which a JetHaler® inhalation device was employed for drug-carrier separation and fine aerosolization. The emitted dose of PFD-RP from capsules and the FPF value were calculated to be 98.6% and 23.4%, respectively. However, ca. 56% of this still remained in the inhalation device or was deposited in the impactor throat and ca. 20% of PFD was deposited in stages 0 and 1. From these physicochemical data, PFD-RP would have an adequate *in vitro* inhalation performance, although further optimization of RP formulation may still be achievable.

Anti-inflammatory Effect on Antigen-evoked Airway Inflammatory Animal Model

In patients with IPF, a significant increase in BAL neutrophils has been noted in 70–90% of patients and the presence of BAL neutrophilia increases the likelihood of underlying fibrotic processes (24). Previously, Beeh and co-workers also demonstrated the established role of neutrophilic inflammation in the pathogenesis of IPF (25). In the present study, to elucidate the therapeutic potential of PFD-RP, the anti-inflammatory effects of insufflated PFD-RP in the respiratory system were assessed using airway inflammatory rats, in which the RP formulation of OVA, an antigen, induced topical inflammatory events in the lung, such as severe neutrophilia and weak eosinophilia (16). At 24 h after antigen insufflation, BALF was obtained to monitor the recruitment of inflammatory cells in the lung (Fig. 3a), since BALF has been frequently used as a biological source for clinical investigation of inflammatory lung diseases (26). Insufflated OVA, an antigen, caused marked recruitment of inflammatory cells in BALF as evidenced by a 6.5-fold increase in total cell numbers, mainly

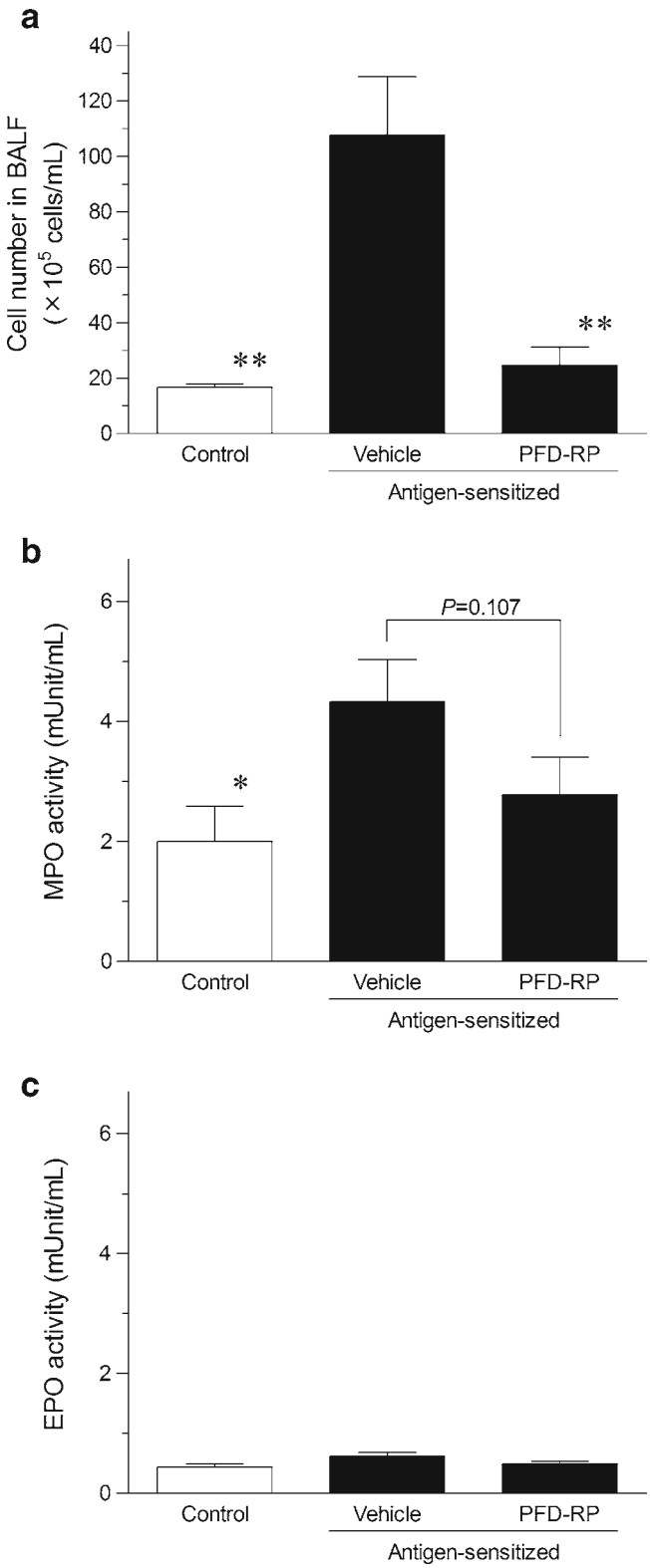

Fig. 3 Anti-inflammatory effects of inhaled PFD-RP in antigen-sensitized rats. At 24 h after the antigen challenge, (**a**) recruited inflammatory cells, (**b**) MPO levels, or (**c**) EPO levels in BALF were monitored in rats with or without pretreatment of PFD-RP (300 μg-PFD/kg). Data represent the mean ± SE of 4–6 determinations. *, $P<0.05$ and **, $P<0.01$ with respect to antigen-sensitized rats with inhaled control-RP.

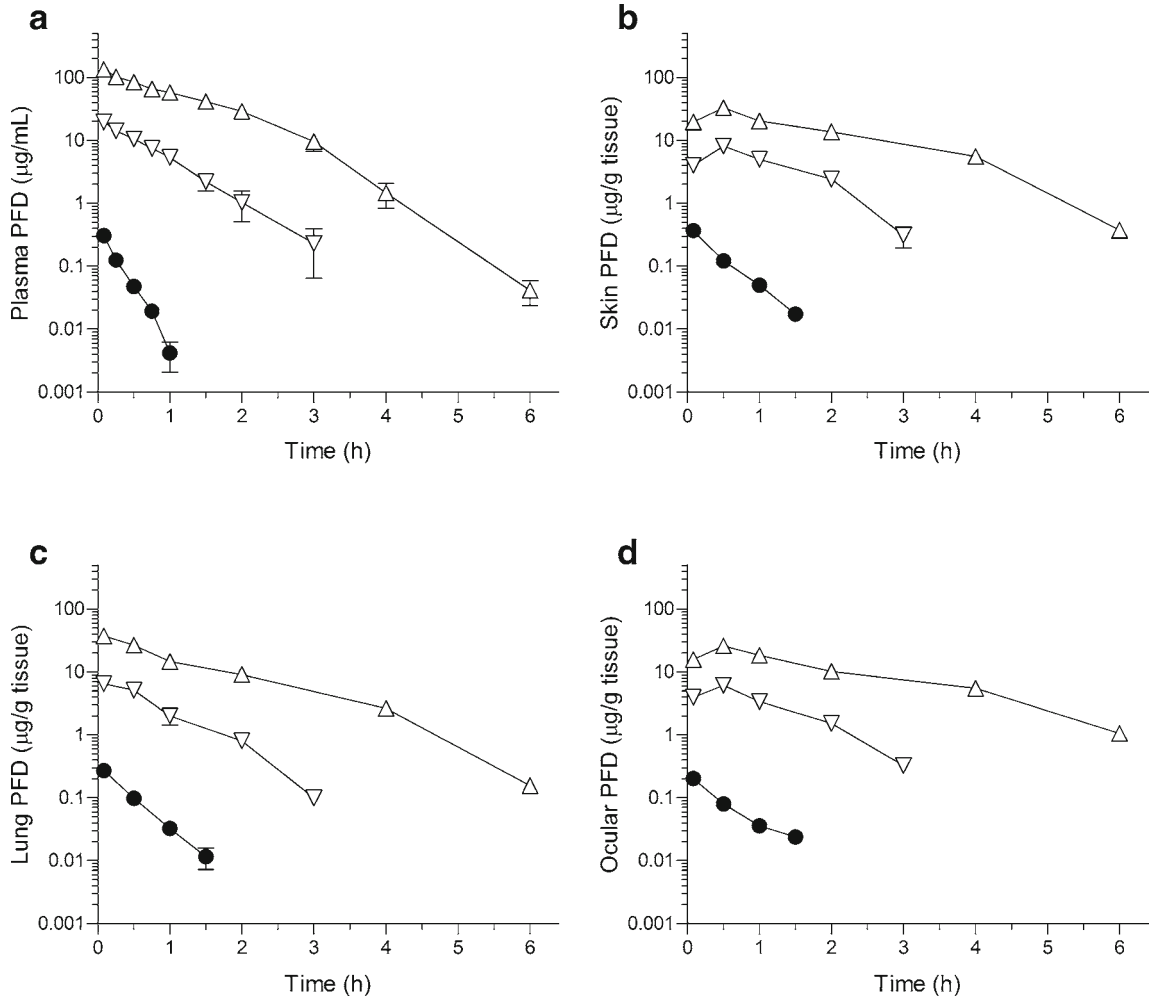

Fig. 4 Concentration-time profiles of PFD in plasma (**a**), skin (**b**), lung (**c**), and eyes (**d**) after intratracheal administration of PFD-RP and oral administration of PFD in rats. ●, insufflated PFD-RP at a pharmacologically effective dose (300 μg PFD/rat); △, orally-taken PFD at a phototoxic dose (160 mg/kg); and ▽, at a non-phototoxic dose (30 mg/kg). Each value represents mean±SE for 4–8 determinations.

consisting of monocytes and neutrophils. In contrast, antigen-evoked airway inflammation seemed to be significantly attenuated by pretreatment with PFD-RP (30–1,000 μg of PFD/rat) in a dose-dependent manner, although PFD-RP at a dose of 100 μg of PFD/rat or lower was found to be less effective. In particular, there appeared to be ca. 90% reduction in infiltrated cells in BALF from sensitized-rats with pretreatment of PFD-RP (300 μg of PFD/rat), and the efficacy of PFD-RP at dose of 1,000 μg-PFD/rat was almost identical to that at 300 μg of PFD/rat in the present experimental model (data not shown). There were no significant differences in the number of recruited cells in BALF between control and antigen-exposed rats with pretreatment of PFD-RP at dose of 300 μg of PFD/rat or much higher. These data were indicative of the therapeutic potential of PFD-RP against airway inflammation and the early symptoms of IPF.

In the development of airway inflammation and fibrotic diseases, MPO and EPO sometimes act as pro-inflammatory and pro-oxidant mediators, mainly released from activated neutrophils/macrophages and eosinophils, respectively (27). These enzymatic activities in BALF have thus been recognized as biomarkers for neutrophilia and eosinophilia. At 24 h after the last antigen challenge, MPO activity in BALF was markedly increased after the OVA challenge (Fig. 3b; 2.00±0.58 and 4.32±0.71 mUnit/mL in non-sensitized and OVA-sensitized rats, respectively), whereas no significant elevations in EPO levels in BALF were seen (Fig. 3c; 0.44±0.05 and 0.62±0.06 mUnit/mL in non-sensitized and OVA-sensitized rats, respectively). From these data, an antigen challenge in the airway system resulted in significant elevations in MPO levels in the lung, suggesting the development of pulmonary neutrophilia in OVA-exposed rats. Pretreatment with PFD-RP (300 μg of PFD/rat) tended to attenuate up-regulation of MPO levels in BALF of OVA-exposed rats by 67%. Not surprisingly, no significant changes in EPO levels were seen even after pre-

treatment with PFD-RP at same dose. Thus, insufflated PFD-RP would be efficacious for suppression of neutrophilic inflammatory symptoms. These observations were in agreement with the inhibitory effects of PFD-RP on the recruitment of inflammatory cells in BALF and the present data could also be indicative of the topical therapeutic potential of PFD-RP for the treatment of pulmonary inflammatory and fibrotic diseases.

In general, localized targeted delivery of drugs into the lungs would offer two primary benefits: (i) reduced nominal dose, which lowers the cost of goods, and (ii) reduced off-target drug exposure, possibly leading to lower systemic side-effects. Previous investigations demonstrated the high therapeutic potential of PFD in several experimental animal models of pulmonary fibrosis, including the anti-fibrotic activity of PFD (p.o., 30 or 100 mg/kg/day) in the bleomycin model of pulmonary fibrosis and the anti-inflammatory effects of PFD (s.c., 500 mg/kg) in an antigen-sensitized model. For the clinical treatment of IPF, PFD was administered orally three times per day with meals, in a total daily dose of 1.8 g, corresponding to ca. 30 mg/kg. In our animal experiments, a pharmacologically effective dose for the RP formulation was deduced to be 300 μg of PFD/rat (ca. 1 mg/kg); however, PFD in systemic administration was found to be effective only at much higher doses. Although a simple and direct comparison on these doses may not be appropriate because of inconsistent experimental conditions, the RP formulation approach would result in marked reductions in the dose of PFD needed to achieve topical pharmacological effects in the lungs.

Pharmacokinetic Behaviour of Pirfenidone after Oral or Intratracheal Administration

From the pharmacological outcomes, reductions in the nominal dose of PFD can be achieved upon the RP formulation strategy; however, de-risk of the phototoxic potential is still unclear. In general, since drug-induced phototoxic responses appear in the skin and eyes, the specific distribution of drug molecules in the skin and/or eyes could be a key consideration for evaluating the phototoxic risk. In the present study, to verify the photosafety of PFD-RP, a pharmacokinetic study on PFD was undertaken after intratracheal administration of PFD-RP at a pharmacologically effective dose (300 μg-PFD/rat). In addition, on the basis of previous findings on phototoxic (160 mg/kg) and non-phototoxic (30 mg/kg) doses in rats (28), pharmacokinetic behaviors of PFD were also characterized after oral administration of a PFD suspension at both doses (30 and 160 mg/kg) for comparison. Concentration-time curves of PFD in the plasma, skin, lung, and eyes were obtained by UPLC/ESI-MS analysis after intratracheal and oral administrations (Fig. 4), and relevant pharmacokinetic parameters of PFD, including C_{max}, $t_{1/2}$, $AUC_{0\rightarrow\infty}$, and MRT, were summarized in Table I. After oral administration of PFD, plasma and lung concentrations of PFD immediately reached the C_{max} within 5 min and these concentrations decreased steadily with half lives of ca. 0.3–0.8 h. With respect to skin and eye depositions, delayed distribution phases were observed, reaching maximum levels at ca. 0.5 h after oral dosing, followed by an elimination phase with a half-life of ca. 0.7–1.1 h. Thus, the elimination of PFD from the skin and eyes was found to

Table I PK Parameters of Plasma and Tissues on PFD in Rats After Oral and Intratracheal Administrations

Samples	C_{max} (plasma, μg/mL; tissues, μg/g tissue)	$t_{1/2}$ (h)	$AUC_{0\rightarrow\infty}$ (plasma, h•μg/mL; tissues, h•μg/g tissue)	MRT (h)
Plasma				
PFD-RP (300 μg-PFD/rat, i.t.)	0.307 ± 0.039	0.17 ± 0.02	0.0835 ± 0.011	0.261 ± 0.011
PFD (30 mg/kg, p.o.)	19.7 ± 0.93	0.33 ± 0.02	14.1 ± 0.92	0.667 ± 0.094
PFD (160 mg/kg, p.o.)	135 ± 11	0.53 ± 0.03	152 ± 10	1.05 ± 0.075
Skin				
PFD-RP (300 μg-PFD/rat, i.t.)	0.369 ± 0.014	0.24 ± 0.02	0.183 ± 0.029	0.427 ± 0.0051
PFD (30 mg/kg, p.o.)	8.16 ± 0.47	1.07 ± 0.28	11.5 ± 0.51	1.14 ± 0.12
PFD (160 mg/kg, p.o.)	32.9 ± 2.6	1.06 ± 0.24	68.0 ± 1.4	1.70 ± 0.043
Lung				
PFD-RP (300 μg-PFD/rat, i.t.)	0.271 ± 0.035	0.28 ± 0.08	0.136 ± 0.039	0.421 ± 0.0080
PFD (30 mg/kg, p.o.)	6.46 ± 0.69	0.80 ± 0.24	6.45 ± 0.43	0.787 ± 0.16
PFD (160 mg/kg, p.o.)	37.6 ± 5.7	0.77 ± 0.16	52.1 ± 1.0	1.32 ± 0.041
Eyes				
PFD-RP (300 μg-PFD/rat, i.t.)	0.202 ± 0.019	0.27 ± 0.06	0.120 ± 0.030	0.554 ± 0.0084
PFD (30 mg/kg, p.o.)	3.95 ± 0.30	0.67 ± 0.18	8.33 ± 0.39	1.06 ± 0.13
PFD (160 mg/kg, p.o.)	26.0 ± 2.6	1.06 ± 0.27	58.8 ± 1.3	1.93 ± 0.051

Each parameter was calculated on the basis of concentration-time curves in plasma and tissues. i.t.: intratracheal administration; and p.o.: oral administration. Each value represents mean ± S.E. for 4–8 rats

be slower than that in plasma and PFD may accumulate in these light-exposed areas (skin and eyes) upon chronic dosing, resulting in an increased phototoxic risk. In contrast, after intratracheal administration of PFD-RP at a pharmacologically effective dose (300 μg-PFD/rat), all plasma and tissue concentrations of PFD immediately reached the C_{max} within 5 min, and then, these concentrations rapidly diminished below detectable levels within 1.5 h. According to estimated PK parameters of PFD in plasma and tissues on the basis of concentration-time curves, C_{max} and $AUC_{0\to\infty}$ values in insufflated PFD-RP at a pharmacologically effective dose (300 μg-PFD/rat) were much lower than those in orally-taken PFD at both phototoxic (160 mg/kg) and non-phototoxic doses (30 mg/kg). In particular, compared with orally-taken PFD at the phototoxic dose, insufflated PFD-RP at the pharmacologically effective dose led to ca. 440-, 90-, and 30-fold reductions in C_{max} values for plasma, skin, and eyes, respectively. The reduced systemic exposure of PFD was also confirmed with decreases in $AUC_{0\to\infty}$ values in plasma, skin, and eyes by ca. 1,800-, 370-, and 440-fold, respectively. In addition, there were still ca. 63–70-fold differences in $AUC_{0\to\infty}$ values for skin and ocular PFD between rats treated with insufflated PFD-RP and orally-taken PFD at non-phototoxic doses (30 mg/kg). From these comparative pharmacokinetic studies, compared with PFD for oral use, the application of the RP system to PFD successfully resulted in marked decreases in skin and eye deposition of PFD, as well as systemic exposure.

In our previous study, the phototoxic potential of fluoroquinolones (FQs) was assessed by *in vitro* phototoxicity assays and an *in vivo* pharmacokinetic study (12). Interestingly, even though most FQs exhibited potent *in vitro* phototoxicity through potent ROS generation under light exposure, FQs with low skin distribution properties were found to be less phototoxic *in vivo*. Thus, the photosafety assessment could be made with combined use of photochemical properties and pharmacokinetic behavior, especially deposition on light-exposed areas. From these previous findings, taken together with the present pharmacokinetic data on PFD, moderate skin disposition upon the RP formulation approach would be efficacious for de-risk of PFD-induced phototoxicity by suppressing excess systemic exposure of PFD. The newly developed PFD-RP system may provide an interesting alternative to oral therapy with a better safety margin for the treatment of IPF. However, since the photosafety of chronic use of PFD-RP is still uncertain, further photosafety assessments may be needed before its clinical use. In addition to the phototoxicity, orally-taken PFD sometimes cause hepatic dysfunction and gastrointestinal side effects such as dyspepsia, nausea and gastroesophageal reflux disease (6,8,9). On the basis of the pharmacokinetic data, these other systemic side-effects might also be attenuated by the newly developed PFD-RP system, because of the limited systemic exposure of PFD after its insufflation. In this context, there may be a need for further comparative studies on (i) toxic biomarkers specific for liver dysfunction and/or gastrointestinal side effects, and (ii) distribution of PFD in gastrointestinal tract and liver. The outcomes from these investigations might provide further support for improved safety of the PFD-RP system in the near future.

CONCLUSION

In the present study, an RP formulation of PFD for the treatment of IPF was firstly prepared to improve photosafety and lower the nominal dose. Photostability testing on PFD formulations demonstrated that PFD-RP, as well as PFD powder, was more highly photostable than that of the PFD solution. PFD-RP also exhibited high dispersibility and suitable particle distribution for inhalation therapy. In antigen-sensitized inflammatory-model rats, insufflated PFD-RP could attenuate antigen-evoked inflammatory symptoms and neutrophilia in the lung. Most notably, PFD-RP at a pharmacologically effective dose (300 μg-PFD/rat) could reduce the phototoxic potential of PFD because of its lower systemic exposure and distribution to light-exposed tissues than that after oral administration of PFD at a phototoxic dose (160 mg/kg). From these findings, the PFD-RP system may provide efficacious and safe medication for the clinical treatment of IPF.

ACKNOWLEDGMENTS AND DISCLOSURES

Authors are grateful to Shionogi&Co., Ltd. for kindly providing pirfenidone. This work was supported in part by a Grant-in-Aid for Young Scientists (B) (No. 22790043; S. Onoue) from the Ministry of Education, Culture, Sports, Science, and Technology and a Health Labour Sciences Research Grant from The Ministry of Health, Labour, and Welfare, Japan.

REFERENCES

1. Hisatomi K, Mukae H, Sakamoto N, Ishimatsu Y, Kakugawa T, Hara S, *et al.* Pirfenidone inhibits TGF-ss1-induced over-expression of collagen type I and heat shock protein 47 in A549 cells. BMC Pulm Med. 2012;12:24.
2. Iyer SN, Gurujeyalakshmi G, Giri SN. Effects of pirfenidone on transforming growth factor-beta gene expression at the transcriptional level in bleomycin hamster model of lung fibrosis. J Pharmacol Exp Ther. 1999;291:367–73.
3. Lasky J. Pirfenidone. IDrugs. 2004;7:166–72.
4. Schaefer CJ, Ruhrmund DW, Pan L, Seiwert SD, Kossen K. Antifibrotic activities of pirfenidone in animal models. Eur Respir Rev. 2011;20:85–97.

5. Corbel M, Lanchou J, Germain N, Malledant Y, Boichot E, Lagente V. Modulation of airway remodeling-associated mediators by the antifibrotic compound, pirfenidone, and the matrix metalloproteinase inhibitor, batimastat, during acute lung injury in mice. Eur J Pharmacol. 2001;426:113–21.
6. Hilberg O, Simonsen U, du Bois R, Bendstrup E. Pirfenidone: significant treatment effects in idiopathic pulmonary fibrosis. Clin Respir J. 2012;6:131–43.
7. Richeldi L, Yasothan U, Kirkpatrick P. Pirfenidone. Nat Rev Drug Discov. 2011;10:489–90.
8. Taniguchi H, Ebina M, Kondoh Y, Ogura T, Azuma A, Suga M, *et al.* Pirfenidone in idiopathic pulmonary fibrosis. Eur Respir J. 2010;35:821–9.
9. Carter NJ. Pirfenidone: in idiopathic pulmonary fibrosis. Drugs. 2011;71:1721–1732.
10. Steinand KR, Scheinfeld NS. Drug-induced photoallergic and phototoxic reactions. Expert Opin Drug Saf. 2007;6:431–43.
11. Onoue S, Seto Y, Gandy G, Yamada S. Drug-induced phototoxicity; an early *in vitro* identification of phototoxic potential of new drug entities in drug discovery and development. Curr Drug Saf. 2009;4:123–36.
12. Seto Y, Inoue R, Ochi M, Gandy G, Yamada S, Onoue S. Combined use of *in vitro* phototoxic assessments and cassette dosing pharmacokinetic study for phototoxicity characterization of fluoroquinolones. AAPS J. 2011;13:482–92.
13. Onoue S, Aoki Y, Kawabata Y, Matsui T, Yamamoto K, Sato H, *et al.* Development of inhalable nanocrystalline solid dispersion of tranilast for airway inflammatory diseases. J Pharm Sci. 2011;100:622–33.
14. Onoue S, Sato H, Kawabata Y, Mizumoto T, Hashimoto N, Yamada S. *In vitro* and *in vivo* characterization on amorphous solid dispersion of cyclosporine A for inhalation therapy. J Control Release. 2009;138:16–23.
15. Onoueand S, Tsuda Y. Analytical studies on the prediction of photosensitive/phototoxic potential of pharmaceutical substances. Pharm Res. 2006;23:156–64.
16. Misaka S, Sato H, Yamauchi Y, Onoue S, Yamada S. Novel dry powder formulation of ovalbumin for development of COPD-like animal model: Physicochemical characterization and biomarker profiling in rats. Eur J Pharm Sci. 2009;37:469–76.
17. Onoue S, Kawamura K, Igarashi N, Zhou Y, Fujikawa M, Yamada H, *et al.* Reactive oxygen species assay-based risk assessment of drug-induced phototoxicity: Classification criteria and application to drug candidates. J Pharm Biomed Anal. 2008;47:967–72.
18. Onoue S, Hosoi K, Wakuri S, Iwase Y, Yamamoto T, Matsuoka N *et al.* Establishment and intra-/inter-laboratory validation of a standard protocol of reactive oxygen species assay for chemical photosafety evaluation. J Appl Toxicol:in press (2012). doi:10.1002/jat.2776.
19. Onoue S, Takahashi H, Kawabata Y, Seto Y, Hatanaka J, Timmermann B, *et al.* Formulation design and photochemical studies on nanocrystal solid dispersion of curcumin with improved oral bioavailability. J Pharm Sci. 2010;99:1871–81.
20. Matsudaand Y, Masahara R. Photostability of solid-state ubidecarenone at ordinary and elevated temperatures under exaggerated UV irradiation. J Pharm Sci. 1983;72:1198–203.
21. Onoue S, Hashimoto N, Yamada S. Dry powder inhalation systems for pulmonary delivery of therapeutic peptides and proteins. Expert Opin Ther Patents. 2008;18:429–42.
22. Suarezand S, Hickey AJ. Drug properties affecting aerosol behavior. Respir Care. 2000;45:652–66.
23. Labirisand NR, Dolovich MB. Pulmonary drug delivery. Part I: physiological factors affecting therapeutic effectiveness of aerosolized medications. Br J Clin Pharmacol. 2003;56:588–99.
24. Pesci A, Ricchiuti E, Ruggiero R, De Micheli A. Bronchoalveolar lavage in idiopathic pulmonary fibrosis: what does it tell us? Respir Med. 2010;104 Suppl 1:S70–3.
25. Beeh KM, Beier J, Kornmann O, Buhl R. Neutrophilic inflammation in induced sputum of patients with idiopathic pulmonary fibrosis. Sarcoidosis Vasc Diffuse Lung Dis. 2003;20:138–43.
26. Tzortzaki EG, Tsoumakidou M, Makris D, Siafakas NM. Laboratory markers for COPD in "susceptible" smokers. Clin Chim Acta. 2006;364:124–38.
27. Onoue S, Misaka S, Kawabata Y, Yamada S. New treatments for chronic obstructive pulmonary disease and viable formulation/device options for inhalation therapy. Expert Opin Drug Deliv. 2009;6:793–811.
28. Seto Y, Aoki Y, Inoue R, Kojo Y, Kato M, Onoue S, *et al.* Development of dry powder inhaler system for reducing phototoxic risk. In: Oku N, editor. DDS conference, vol. 20. Shizuoka: Biomedical Research Press; 2011. p. 41–6.